JOURNAL OF GEOPHYSICAL RESEARCH, VOL. 113, D05211, doi:10.1029/2007JD009092, 2008

Predicted change in global secondary organic aerosol concentrations in response to future climate, emissions, and land use change

C. L. Heald,[1,2] D. K. Henze,[3] L. W. Horowitz,[4] J. Feddema,[5] J.-F. Lamarque,[6] A. Guenther,[6] P. G. Hess,[6] F. Vitt,[6] J. H. Seinfeld,[3] A. H. Goldstein,[1] and I. Fung[1]

Received 22 June 2007; revised 3 October 2007; accepted 29 November 2007; published 11 March 2008.

[1] The sensitivity of secondary organic aerosol (SOA) concentration to changes in climate and emissions is investigated using a coupled global atmosphere-land model driven by the year 2100 IPCC A1B scenario predictions. The Community Atmosphere Model (CAM3) is updated with recent laboratory determined yields for SOA formation from monoterpene oxidation, isoprene photooxidation and aromatic photooxidation. Biogenic emissions of isoprene and monoterpenes are simulated interactively using the Model of Emissions of Gases and Aerosols (MEGAN2) within the Community Land Model (CLM3). The global mean SOA burden is predicted to increase by 36% in 2100, primarily the result of rising biogenic and anthropogenic emissions which independently increase the burden by 26% and 7%. The later includes enhanced biogenic SOA formation due to increased emissions of primary organic aerosol (5–25% increases in surface SOA concentrations in 2100). Climate change alone (via temperature, removal rates, and oxidative capacity) does not change the global mean SOA production, but the global burden increases by 6%. The global burden of anthropogenic SOA experiences proportionally more growth than biogenic SOA in 2100 from the net effect of climate and emissions (67% increase predicted). Projected anthropogenic land use change for 2100 (A2) is predicted to reduce the global SOA burden by 14%, largely the result of cropland expansion. South America is the largest global source region for SOA in the present day and 2100, but Asia experiences the largest relative growth in SOA production by 2100 because of the large predicted increases in Asian anthropogenic aromatic emissions. The projected decrease in global sulfur emissions implies that SOA will contribute a progressively larger fraction of the global aerosol burden.

Citation: Heald, C. L., et al. (2008), Predicted change in global secondary organic aerosol concentrations in response to future climate, emissions, and land use change, *J. Geophys. Res.*, *113*, D05211, doi:10.1029/2007JD009092.

1. Introduction

[2] Organic carbon aerosol is a dominant component of observed submicron particulate matter, with contributions ranging from 20 to 90% [*Kanakidou et al.*, 2005]. These aerosols can be directly emitted (primary) or formed in the atmosphere (secondary) following the oxidation of volatile organic compounds (VOC). Precursors of secondary organic aerosols (SOA) include both anthropogenic and biogenic compounds, emissions of which are expected to rise as a consequence of human activities and increasing global temperatures [*Intergovernmental Panel on Climate Change* (*IPCC*), 2007]. Climatic conditions also control SOA concentrations in the atmosphere via temperature, precipitation and the oxidative capacity of the atmosphere. SOA contributes both to air quality degradation and climate forcing, however their impact relative to other aerosols remains highly uncertain [*Kanakidou et al.*, 2005]. We investigate here the sensitivity of the atmospheric burden of SOA to changes in climate, emissions and land use change predicted for the year 2100.

[3] The yields of SOA from the condensation of semivolatile oxidation products of VOCs have been extensively studied in laboratory chambers. Organic aerosol growth has been observed following the oxidation of biogenic terpenoid compounds (monoterpenes and sesquiterpenes) [*Griffin et al.*, 1999; *Lee et al.*, 2006a, 2006b] and anthropogenic aromatics such as toluene and xylene [*Odum et al.*, 1997; *Jang and Kamens*, 2001; *Kleindienst et al.*, 2004]. *Kroll et al.* [2005, 2006] demonstrated that isoprene photooxidation leads to aerosol formation. Isoprene is the most abundantly emitted VOC compound (~500 Tg C a^{-1} [*Guenther et al.*,

[1]Department of Environmental Science, Policy and Management, University of California, Berkeley, California, USA.
[2]Now at Department of Atmospheric Science, Colorado State University, Fort Collins, Colorado, USA.
[3]Department of Chemical Engineering, California Institute of Technology, Pasadena, California, USA.
[4]Geophysical Fluid Dynamics Laboratory, NOAA, Princeton, New Jersey, USA.
[5]Department of Geography, University of Kansas, Lawrence, Kansas, USA.
[6]National Center for Atmospheric Research, Boulder, Colorado, USA.

0148-0227/08/2007JD009092$09.00

1995]) and therefore, despite low SOA yields (1–3%), may make up an important fraction of SOA formed in the atmosphere [*Henze and Seinfeld*, 2006]. On the basis of low yields, anthropogenic SOA formation was thought to be negligible outside of urban centers [*Tsigaridis and Kanakidou*, 2003]; however recent studies have identified additional anthropogenic SOA sources (i.e., benzene [*Martin-Reviejo and Wirtz*, 2005]) and have documented enhanced anthropogenic SOA yields, particularly in the presence of low nitrogen oxide concentrations [*Ng et al.*, 2007a].

[4] Despite well-studied laboratory systems, ambient observations of organic carbon aerosol indicate that the global SOA budget is not well understood. Surface OC aerosol concentrations in Mexico City [*Volkamer et al.*, 2006] and off the coast of New England [*de Gouw et al.*, 2005] suggest an underestimate in the anthropogenic SOA source. A factor of 10–100 underestimate in OC aerosol concentrations observed in the free troposphere off of Asia is attributed to an underestimate in secondary production [*Heald et al.*, 2005]. Surface concentrations of OC aerosol in rural England [*Johnson et al.*, 2006] and within a laboratory chamber [*Johnson et al.*, 2005] could only be reproduced by increasing aerosol-gas partitioning coefficients for SOA 5–500 fold. Numerous factors could contribute to these discrepancies between models and observations, including: additional classes of SOA precursors, more efficient SOA formation in ambient conditions relative to yields measured in laboratory chambers, biases in global model predictions of SOA (for example, in precursor emission inventory estimates), and additional SOA formation mechanisms. In addition to condensation of semivolatile oxidation products, formation mechanisms relevant to global budgets may include heterogeneous reactions of organic compounds [*Kroll et al.*, 2005; *Liggio et al.*, 2005], cloud processing [*Lim et al.*, 2005; *Carlton et al.*, 2006] and oligomerization [*Gao et al.*, 2004; *Kalberer et al.*, 2004]. The range of chemical and physical environments represented by these studies suggests that the mechanisms and precursors contributing to SOA formation are diverse. In light of these discrepancies, previous estimates of the global source of SOA (12–40 Tg C a^{-1} [*IPCC*, 2001]) are likely to be an underestimate. *Goldstein and Galbally* [2007] show that carbon mass balance could allow for up to an order of magnitude greater SOA in the atmosphere. Additional observations, particularly in the Southern Hemisphere, are required to constrain these budgets.

[5] Global models have been used to simulate the formation of SOA from the condensation of semivolatile VOC oxidation products based on gas-particle partitioning theory parameterization of laboratory chamber yields [*Chung and Seinfeld*, 2002; *Tsigaridis and Kanakidou*, 2003; *Lack et al.*, 2004; *Henze and Seinfeld*, 2006]. *Tsigaridis et al.* [2006] explore how aerosol composition, including SOA, has changed since preindustrial times. *Liao et al.* [2006] predict a 54% increase in SOA from terpene oxidation in 2100 as a result of changes in climate and anthropogenic emissions from the IPCC A2 emission scenario. *Tsigaridis and Kanakidou* [2007] use a chemical transport model to investigate how SOA responds to emissions changes in the IS92a scenario, and predict more than a doubling of the global SOA burden. Here we employ the National Center for Atmospheric Research (NCAR) Community Atmospheric Model with chemistry (CAM-Chem) including the latest laboratory measurements of biogenic and anthropogenic SOA yields, in conjunction with the Community Land Model (CLM) to simulate global SOA formation under present and future climate.

[6] A number of model studies have examined chemistry-climate interactions and the sensitivity of tropospheric composition to future projections [*Stevenson et al.*, 2000; *Grewe et al.*, 2001; *Grenfell et al.*, 2003; *Zeng and Pyle*, 2003; *Liao et al.*, 2006; *Chen et al.*, 2007]. *Brasseur et al* [2006], using the same chemical model employed here (MOZART), found that changes in oxidant concentrations in 2100 resulted primarily from changing anthropogenic emission rates, water vapor concentrations and lightning emissions. *Murazaki and Hess* [2006] examined the effect of changing climatic conditions on surface ozone using the same meteorological-chemical model coupling employed here. *Sanderson et al* [2003] used a coupled vegetation–atmosphere model to predict changes in isoprene and ozone in a future climate. Historical climate and CO_2 concentrations have been used to investigate the climate sensitivity of isoprenoid emissions over the past decades [*Naik et al.*, 2004; *Tao and Jain*, 2005].

[7] The purpose of this study is to build on these previous examinations of emission response and chemistry-climate interactions to investigate how SOA formation is predicted to respond to climate, emissions and anthropogenic land use changes under the IPCC Special Report on Emissions Scenario (SRES). We focus here on projections using the A1B scenario, but offer comparisons with the A2, or business as usual, scenario to highlight potentially large sensitivities where appropriate. Although SOA models may be incomplete, they include our best understanding of SOA formation and the key parameters to which we expect SOA concentrations to respond (precursor emissions, oxidation, condensation on preexisting aerosol mass, temperature sensitive gas-aerosol partitioning and removal via precipitation). We employ a global climate model here to capture the effect of climate change on SOA, but we do not address the feedback of SOA on climate (through the direct or indirect effect). We aim to highlight the main drivers for predicted change in SOA burden and identify sensitivities which need to be examined further in the laboratory. We focus here on the relative changes in global SOA budget and geographical distributions predicted relative to the present day and leave an assessment of climate forcings and feedbacks to future studies when the total SOA budget and SOA optical properties can be assessed with a greater degree of certainty.

2. Model Description

2.1. Community Atmospheric Model

[8] The global NCAR Community Atmospheric Model (CAM3) is a part of the Community Climate System Model (CCSM3) [*Collins et al.*, 2006a, 2006b]. We employ CAM3 here in its stand-alone atmospheric general circulation model (AGCM) mode integrated with the Community Land Model (see section 2.3). This model includes a simulation of O_3-NO_x-CO-VOC and aerosol phase chemistry based on

the MOZART (Model of Ozone and Related Chemical Tracers) chemical transport model [*Tie et al.*, 2001, 2005; *Horowitz et al.*, 2003; *Lamarque et al.*, 2005]. The MOZART model has been applied in a suite of tropospheric composition studies; the most recent evaluations of the model with observations are given by *Kinnison et al.* [2007] and *Ginoux et al.* [2006]. The coupled CAM-Chem system has previously been used to examine aerosol forcing in a future climate [*Lamarque et al.*, 2005]. Simulations are performed here with a 30 minute time step and a horizontal resolution of $2^\circ \times 2.5^\circ$ with 26 vertical levels from the surface to the lower stratosphere ($\sim$4 Pa).

[9] Simulated aerosol mass classes include sulfate from the oxidation of SO_2 (both emitted directly and from DMS oxidation), ammonium nitrate, directly emitted carbonaceous aerosols (black carbon, organic carbon), secondary organic aerosols, sea salt and dust. All aerosols are considered to be externally mixed. Carbonaceous aerosols are emitted as 80% hydrophobic and 20% hydrophilic in the case of BC, and 50% hydrophobic and 50% hydrophilic for primary OC [*Tie et al.*, 2005]. Hydrophobic aerosols are converted to hydrophilic form to account for aerosol aging and mixing with an e-folding time of 1.15 d [*Cooke et al.*, 1999]. This fixed timescale does not account for varying atmospheric oxidant concentrations. We scale primary organic aerosol concentrations by a factor of 2 to account for noncarbon mass [*Turpin and Lim*, 2001].

[10] Secondary organic aerosol formation in CAM-Chem follows the 2-product model of *Odum et al.* [1997] where two semivolatile products (P) are formed from the oxidation of a parent hydrocarbon (HC) by an oxidant (OX) with mass-based stoichiometric yields (α)

$$HC + OX \rightarrow \alpha_1 P_1 + \alpha_2 P_2 \tag{1}$$

The partitioning of these products between the aerosol (A_i) and gas phase (G_i) is dictated by absorptive partitioning theory into an organic material [*Pankow*, 1994], where the partitioning coefficient ($K_{om,i}$) for each semivolatile compound (i), is given by:

$$K_{om,i} = \frac{A_i}{G_i M_o} \tag{2}$$

M_o is the amount of preexisting organic aerosol mass upon which SOA can condense; here M_o consists of both primary organic aerosol (POA) and SOA, thus SOA formation is nonlinear. As described by *Chung and Seinfeld* [2002] this mass balance is calculated by iteratively solving the following (bisectional iteration is employed here):

$$\sum_i \left[\frac{K_{om,i,1}\left(\alpha_{i,1}\Delta HC_i + A^0_{i,1} + G^0_{i,1}\right)}{\left(1 + K_{om,i,1}M_o\right)} + \frac{K_{om,i,2}\left(\alpha_{i,2}\Delta HC_i + A^0_{i,2} + G^0_{i,2}\right)}{\left(1 + K_{om,i,2}M_o\right)} \right] + \frac{[POA]}{M_o} = 1 \tag{3}$$

where A^0_i and G^0_i describe the initial aerosol and gas in each grid cell, such that at every time step, the semivolatile products repartition to establish equilibrium. The gas phase semivolatiles (G_i) are transported and deposited following *Chung and Seinfeld* [2002].

[11] The mass-based stoichiometric yields (α_i) and the partitioning coefficients ($K_{om,i}$) for a high-volatility and a low-volatility product are empirically derived from measured VOC oxidation experiments. We include biogenic SOA from the oxidation of monoterpenes by OH, O_3 and NO_3 according to the yields of *Griffin et al.* [1999], as adapted by *Chung and Seinfeld* [2002] for the pinene class of precursors, and the photooxidation by OH of isoprene under low nitrogen oxide (NO_x) conditions estimated by *Kroll et al.* [2006]with yield parameters from *Henze and Seinfeld* [2006]. Anthropogenic SOA from the oxidation of aromatics (benzene, toluene and xylene) by OH is included on the basis of recent results of *Ng et al.* [2007a]. These yields are sensitive to NO_x concentrations and we follow the treatment of *Henze et al.* [2008] to simulate the formation of SOA from the reaction of aromatic oxidation products with peroxy radicals (HO_2) or nitric oxide (NO). In this formulation, aromatic oxidation products in low NOx conditions are essentially nonvolatile. Although short-lived sesquiterpenes and oxygenated VOCs (>C6) have been shown to produce SOA [*Griffin et al.*, 1999], a lack of speciated global emissions estimates for these compounds precludes including them in the vegetation model here.

[12] The partitioning coefficients vary directly with temperature and indirectly via temperature-sensitive vapor pressure as described by the Clausius-Clapeyron equation. We use an enthalpy of vaporization of 42 kJ mol^{-1} following *Chung and Seinfeld* [2002], which also matches the effective enthalpy estimated for products of α-pinene oxidation [*Offenberg et al.*, 2006] and isoprene oxidation [*Kleindienst et al.*, 2007]. Estimates reported for the enthalpy of vaporization of aromatic SOA vary from 15 kJ mol^{-1} [*Offenberg et al.*, 2006] to 48 kJ mol^{-1} [*Takekawa et al.*, 2003]. There is not yet sufficient evidence to support the use of more than a single value for the simulations performed here. A sensitivity test where the enthalpy of vaporization for aromatic compounds is reduced to 15 kJ mol^{-1} results in a 21% reduction in aromatic SOA production; we note that this decreased sensitivity to temperature would diminish the sensitivity of SOA to future climate.

[13] Nitrogen oxide concentrations have recently been recognized as an important control on SOA formation efficiency [*Kroll et al.*, 2005; *Presto et al.*, 2005; *Song et al.*, 2005]. The implementation of aromatic SOA formation followed here [*Henze et al.*, 2008] explicitly assesses the competition between low and high NOx pathways. We examine how the NO_x/VOC ratio, and therefore the SOA production efficiency, is predicted to change in the future in section 4.

[14] Removal of species occurs by both dry and wet deposition. Dry deposition follows a resistance-in-series formulation [*Wesely*, 1989]. Wet deposition of gas phase components is simulated as a first-order loss process based on the large-scale and convective precipitation rates [*Rasch et al.*, 1997; *Horowitz et al.*, 2003]. Soluble gaseous species are removed by in-cloud scavenging [*Giorgi and Chameides*, 1985] and below-cloud washout [*Brasseur et al.*, 1998]. Soluble aerosols (sulfate, hydrophilic organic carbon, hydrophilic black carbon, SOA) are similarly

Table 1. List of Simulations[a]

	2000	2100A	2100Aa	2100Ao	2100B	2100C	2100A2	2100ABC	2000L	2100L
Mapped emission factors	●	●	●	●	●	●	●	●		
2000										
Climate	●	●	●	●	●		●		●	●
Vegetation	●	●	●	●	●	●	●	●	●	
Biogenic emissions	●	●	●	●		●	●		●	●
POA emissions	●		●		●	●			●	●
Aromatic emissions	●			●	●	●			●	●
Other anthropogenic emissions	●		●	●	●	●			●	●
2100 (A1B)						●		●		
Vegetation										●
Biogenic emissions					●			●		
POA emissions		●		●				●		
Aromatic emissions		●	●					●		
Other anthropogenic emissions		●						●		
2100 (A2)										
POA emissions							●			
Aromatic emissions							●			
Other anthropogenic emissions							●			

[a]Dots specify parameters selected for each simulation.

removed in-cloud by rain and below-cloud by both rain and snow [*Barth et al.*, 2000]. We note here that evaluations of the CAM3 precipitation with GPCP observations indicate that precipitation is overestimated in the tropics and underestimated in the subtropics [*Collins et al.*, 2006b] which will inversely affect aerosol lifetimes.

[15] Future climate simulations for the year 2100 are driven by carbon dioxide concentrations specified for the IPCC SRES A1B scenario [*IPCC*, 2001]. The transient climate sensitivity of the CCSM3 fully coupled model is 2.47°C [*Kiehl et al.*, 2006]. We do not investigate the effect of SOA on the radiation budget and therefore specify fixed sea surface temperatures archived from previous NCAR CCSM climate change experiments using the SRES A1B emissions [*Meehl et al.*, 2006]. Globally averaged temperature increases here by 1.8°C by 2100 for A1B. A full analysis of the CCSM3 future climate simulation is not the objective of this work, see *Meehl et al.* [2006] for further details.

[16] For this study we performed 10 simulations. For future simulations, we modify one parameter at a time, labeling these simulations for their future conditions: anthropogenic emissions (2100A), biogenic emissions (2100B), climate (2100C), and anthropogenic land use (2100L). In addition, a number of sensitivity simulations were performed to separate the effects of different anthropogenic emissions (Table 1). Each model simulation is initialized with a 1-year spin-up run. Following initialization, present-day simulations are performed for 1 year, future ''snapshot'' climate simulations are performed for 10 years and results are averaged to estimate the effect of interannual climate variability.

2.2. Anthropogenic Emissions

[17] Emissions of both gas and aerosol phase species for the years 2000 and 2100 are taken from *Horowitz* [2006]. Present-day (2000) fossil fuel emissions are from the EDGAR v2.0 inventory [*Olivier et al.*, 1996], with the exception of speciated aromatics, which are taken from the RETRO inventory [*van het Bolscher et al.*, 2007], and OC and BC, which follow *Cooke et al.* [1999]. *Cooke et al.* [1999] recommend scaling anthropogenic OC emissions by a factor of 2 to account for SOA; unlike *Horowitz* [2006], we do not include this scaling here. Biomass burning emissions for all species are from *Hao and Liu* [1994] in the tropics and *Muller* [1992] in the extratropics, again with the exception of the aromatics taken from RETRO [*Schultz et al.*, 2008]. The biogenic emissions are described in section 2.3.

[18] Anthropogenic emissions for future simulations (2100) are constructed on the basis of the IPCC SRES [*Nakicenov et al.*, 2000]. *Horowitz* [2006] apply scaling factors to fossil fuel sources and 50% of biomass burning emissions from the year 2000. Resulting emissions for POA and SOA-precursors corresponding to the A1B and A2 marker scenarios used here are given in Table 2. These scenarios are based on different socioeconomic assumptions and predict relatively moderate and high growth in emissions respectively. Figure 1 shows the geographical distribution of emissions of POA and aromatics (benzene, toluene and xylene) for 2000 and the projected change in 2100 according to the A1B scenario. This scenario predicts a global increase in POA emissions of 60% by 2100, whereas an initial increase in aromatic emissions from the year 2000 is followed by a decline, with 2100 emissions predicted to be 27% higher than 2000. The A2 scenario predicts much larger increases in global aromatic emissions of 118%. All of these scenarios predict large relative growth in Asian emissions, where even the A1B scenario predicts

Table 2. Total Emissions of SOA Precursors, Primary OC, and Nitrogen Oxides (NOx)

Species	2000 Emissions	2100: A1B	2100: A2
Monoterpenes, Tg C a^{-1}	43	51 (+19%)	not simulated[a]
Isoprene, Tg C a^{-1}	496	607 (+22%)	not simulated[a]
Aromatics,[b] Tg C a^{-1}	16.0	20.3 (+27%)	34.9 (+118%)
POA, Tg C a^{-1}	45	72 (+60%)	96 (+113%)
NOx, Tg N a^{-1}	41	48 (+17%)	112 (+172%)

[a]The A2 climate was not simulated here, therefore an estimate for A2 BVOC emissions in 2100 is not provided.
[b]Sum of benzene, toluene and xylene.

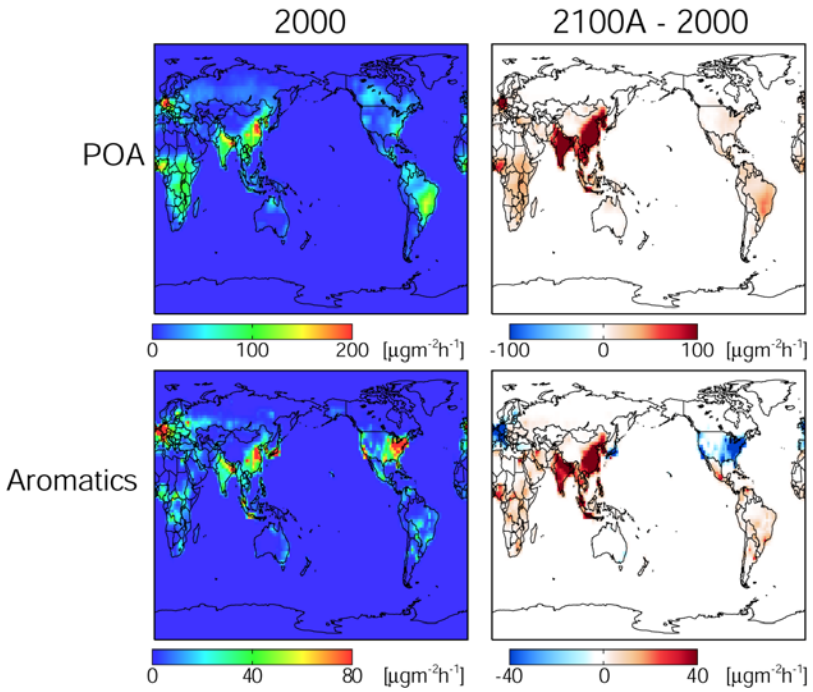

Figure 1. Global emission of primary organic carbon aerosol (POA) and total aromatics (benzene, toluene and xylene) for 2000 and the change in emissions predicted between 2100 and 2000 according to the SRES A1B marker scenario (2100A). Color scales are saturated at respective values.

more than a doubling of aromatic and POA emissions by 2100.

2.3. Community Land Model and Biogenic VOC Emissions

[19] The NCAR Community Land Model (CLM3) is the component of the CCSM3 [*Collins et al.*, 2006a] which simulates the biogeophysical processes associated with land-atmosphere exchange [*Dickinson et al.*, 2006]. Vegetation is described by 16 plant functional types (PFTs). Land surface parameters (including leaf area index, LAI) are consistent with MODIS land surface data sets [*Lawrence and Chase*, 2007]. The CLM can also simulate dynamic vegetation which responds to climate variations [*Bonan et al.*, 2002]. The model is used here with the same spatial and temporal resolution of the CAM3 model (section 2.1) in the prescribed vegetation mode.

[20] We have implemented the biogenic volatile organic compound (BVOC) emission models of *Guenther et al.* [1995, 2006] into the CLM3. These emissions models, referred to as G95 and MEGAN2 (Model of Emissions of Gases and Aerosols from Nature, version 2.0) respectively, were derived from field and laboratory studies. Canopy-level fluxes of each terrestrial BVOC (i) in units of [μg C m^{-2} h^{-1}] are estimated according to:

$$F_i = \gamma_i \rho \sum_j \varepsilon_{i,j} \chi_j \qquad (4)$$

where, $\varepsilon_{i,j}$ is the emission factor at standard conditions of light, temperature and leaf area for vegetation type j with fractional areal coverage χ_j, γ_i is the emission activity factor which accounts for emission responses to meteorological and phenological conditions and ρ is the canopy loss and production factor (set here to unity as recommended for isoprene by *Guenther et al.* [2006]).

[21] Emissions of monoterpenes follow the G95 treatment as implemented by *Levis et al.* [2003]. Plant-dependent emission capacities are specified for each plant functional type within a grid box [μg C g^{-1} h^{-1}], multiplied by grid box specific foliar densities [g m^{-2}], and scaled by an exponential function of leaf temperature as calculated within CLM3. The 6 plant functional types specified in G95 are mapped to the 16 CLM plant functional types as shown in Table 3.

[22] Emissions of isoprene follow MEGAN2 with detailed canopy light and temperature algorithms [*Guenther et al.*, 2006]. Emission factors [in units of flux, μg C m^{-2} h^{-1}] are geographically mapped for each plant functional type,

Table 3. Plant Functional Types in CLM and MEGAN

CLM Plant Functional Type	MEGAN Plant Function Type
Needleleaf evergreen tree, temperate	fineleaf evergreen trees
Needleleaf evergreen tree, boreal	fineleaf evergreen trees
Needleleaf deciduous tree	fineleaf deciduous trees
Broadleaf evergreen tree, tropical	broadleaf trees
Broadleaf evergreen tree, temperate	broadleaf trees
Broadleaf deciduous tree, tropical	broadleaf trees
Broadleaf deciduous tree, temperate	broadleaf trees
Broadleaf deciduous tree, boreal	broadleaf trees
Broadleaf evergreen shrub	shrubs
Broadleaf deciduous shrub, temperate	shrubs
Broadleaf deciduous shrub, boreal	shrubs
C3 grass, arctic	grasses
C3 grass, non-arctic	grasses
C4 grass	grasses
Corn	crops
Wheat	crops

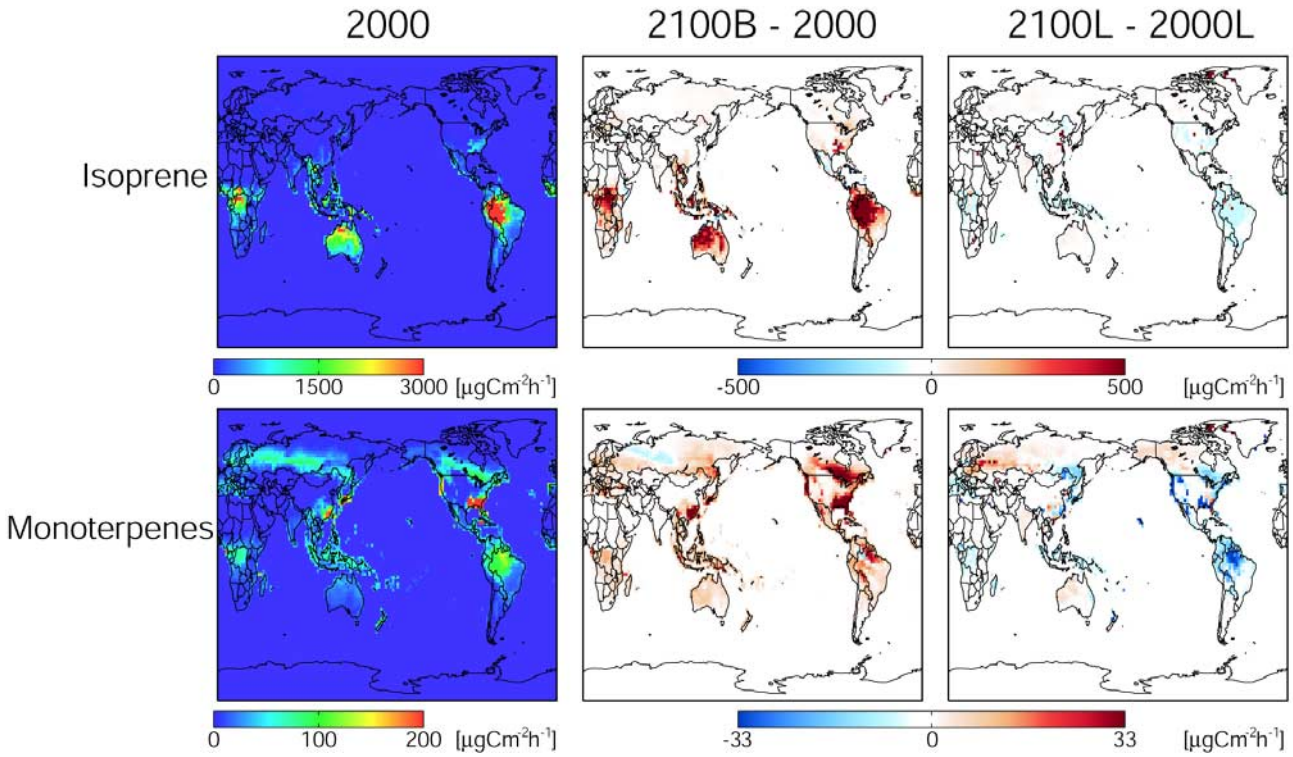

Figure 2. (left) Terrestrial biogenic volatile organic compounds (BVOC) emissions simulated using the G95 (monoterpenes) and MEGAN (isoprene) algorithms within the Community Land Model for the year 2000 and the change in emissions predicted between 2100 and 2000, due to (middle) climate (2100B) and (right) land use change (2100L). Color scales are saturated at respective values.

reflecting species-wide divergence in emission capacities. The same PFT mapping implemented for G95 applies here. The isoprene activity factor includes scalings for light (γ_P), temperature (γ_T), leaf age (γ_{age}), soil moisture (γ_{SM}) and leaf area index (LAI):

$$\gamma = C_{CE} LAI \gamma_P \gamma_T \gamma_{age} \gamma_{SM} \quad (5)$$

The activity factors in equation (5) are calculated on the basis of the instantaneous temperature, radiation, soil moisture and LAI at each time step in the CLM, as well as the average temperature and radiation conditions over the last 24 h and 10 d. The radiation response is applied separately for the sunlit and shaded leaves in the forest canopy environment. We derive a canopy environment constant (C_{CE}), a factor used to set emission activity to unity at standard conditions, of 0.40 for the CLM model at the standard conditions specified by *Guenther et al.* [2006].

[23] Emissions of monoterpenes and isoprene calculated interactively for the years 2000 and 2100 are shown in Figure 2, and totals are given in Table 2. Isoprene emissions estimated here for the year 2000 (496 Tg C a^{-1}) are consistent with previous estimates from *Guenther et al.* [1995, 2006] (440–660 Tg C a^{-1}). Monoterpene emissions (43 Tg C a^{-1}) are at the low end of the reported range of previous studies (33–147 Tg C a^{-1}) [*Muller*, 1992; *Guenther et al.*, 1995; *Levis et al.*, 2003; *Naik et al.*, 2004; *Tao and Jain*, 2005]. Differences are primarily attributed to vegetation cover and LAI and are within the uncertainty of estimated emissions [*Shim et al.*, 2005; *Guenther et al.*, 2006].

[24] Biogenic emissions are simulated to increase by 22% in 2100 when greenhouse gas concentrations follow the A1B scenario. These percentage increases in emissions are globally distributed and primarily driven by a 1.8°C global mean increase in surface temperature simulated here. Global mean radiation, cloud fraction, and soil moisture are within 5% of 2000 values. Western Siberia experiences a projected summertime reduction in temperature in 2100 resulting in a slight decrease in isoprene emissions. A study based on the G95 algorithms predicts a 34% increase in isoprene emission when surface temperature increases by 4.7°C and vegetation is fixed [*Sanderson et al.*, 2003].

[25] Many factors that may influence biogenic emissions are not included in current emission algorithms, largely because of insufficient data [*Guenther et al.*, 2006]. Increases in carbon dioxide concentrations above ambient have been shown to inhibit leaf isoprene production, as summarized by *Arneth et al.* [2007], however only a limited number of plant species in limited conditions have been examined. *Possell et al.* [2005] synthesized the studies to date to estimate a CO_2 isoprene inhibition factor, suggesting that a relative increase in CO_2 concentrations to 2100 levels (from 369 ppb to 717 ppb) based on the A1B scenario, would cause a 49% decrease in isoprene emission. Increases in carbon dioxide concentrations could also fertilize vegetation [*Drake et al.*, 1997; *Korner*, 2000]; enhanced plant growth may globally counteract a decrease in emission rate. Isoprene emissions have also been shown to respond to

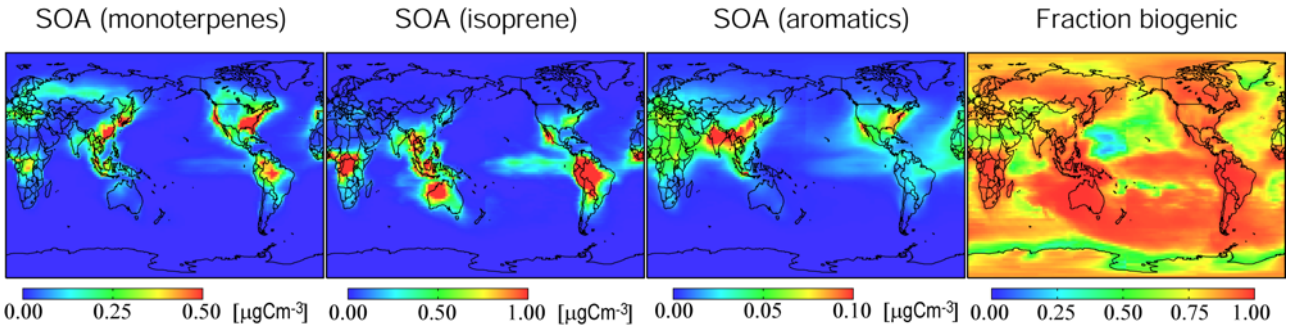

Figure 3. Annual mean simulated surface SOA concentrations for the year 2000. SOA from each precursor is shown separately. The fourth panel shows the fraction of SOA from biogenic precursors (isoprene+monoterpenes). The color scales are saturated.

acute ozone exposure [*Velikova et al.*, 2005], although the effects of chronic exposure are unclear. Monoterpene emissions may be similarly sensitive to ozone concentrations [*Loreto et al.*, 2004]. Biogenic emissions are also likely affected by nutrient availability and physical stress [*Harley et al.*, 1994; *Alessio et al.*, 2004]. Future biogenic emission projections are therefore highly uncertain and reflect only the subset of robust meteorological relationships observed and included in emission algorithms.

3. Results

3.1. Present-Day Simulation of SOA

[26] Figure 3 shows the annual mean simulated concentrations of SOA at the surface for the present day (2000). The geographical distribution reflects precursor emissions, with anthropogenic SOA in Asia, Europe and the northeastern United States, and large concentrations of biogenic (isoprene) SOA in the tropics and in the southeastern United States in local summer. SOA from monoterpenes is most important in the boreal regions in summertime. SOA at the surface is 20–90% biogenic, strongly dependent on season and region.

[27] The vertical distribution of SOA simulated here is shown in Figure 4. SOA concentrations peak at the surface because of the proximity to emissions of precursors, with lifetimes on the order of hours against oxidation, and the abundance of POA as condensation sites. However, SOA condensation is favored at cold temperatures, and thus precursors aloft can efficiently be converted to aerosol form, providing an in situ free tropospheric source, unlike POA. Rapid precursor oxidation generally limits SOA from monoterpenes to the lower troposphere. *Henze and Seinfeld* [2006] find that isoprene is generally not completely oxidized at the source because of large emissions, and thus that oxidation away from sources and vertical lofting enhance the burden aloft of SOA from isoprene compared to monoterpene SOA. Less precipitation at altitude gives rise to longer soluble aerosol lifetimes [*Balkanski et al.*, 1993], ~9 d (global mean) for isoprene SOA compared to 7 d for SOA from monoterpene sources. SOA from aromatic precursors exhibits an intermediate vertical extent, with a corresponding global mean lifetime of 8 d.

[28] Figure 5 shows the net seasonal production of SOA (formation – reevaporation) from the three precursor classes; totals are given in Table 4. Global production is dominated by isoprene (19 Tg C a^{-1}), with over half of annual isoprene production taking place in the Southern Hemisphere due primarily to the forested regions of the Amazon and southern Africa. Over 75% of the anthropogenic production (global total 1.4 Tg C a^{-1}) takes place in the Northern Hemisphere, which is hemispherically aseasonal, but varies locally [*Henze et al.*, 2008]. Emissions of monoterpenes simulated here are roughly half of previous estimates (section 2.3), resulting in a small contribution (global production 3.7 Tg C a^{-1}) to total simulated SOA. SOA production in present-day totals 24.3 Tg C a^{-1}, with a global annual mean burden of 0.59 Tg C. *Henze et al.*

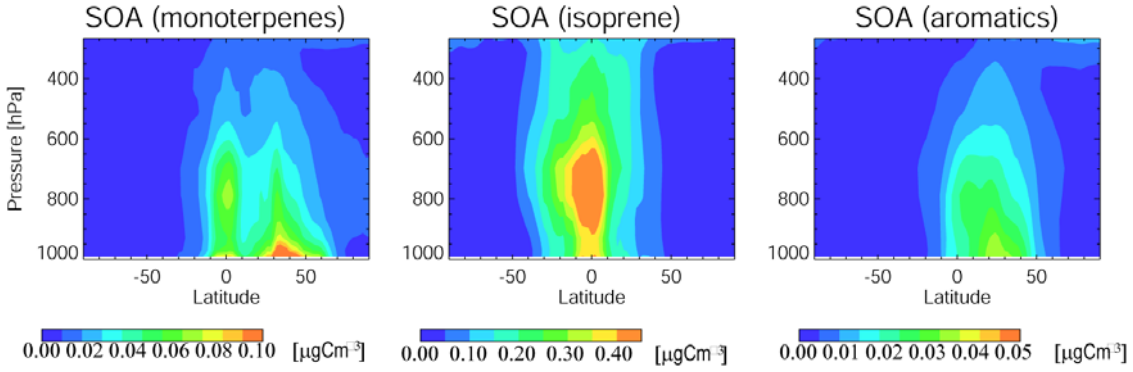

Figure 4. Annual mean zonal distribution of simulated SOA concentrations from each precursor for the year 2000. Color scales are saturated at respective values.

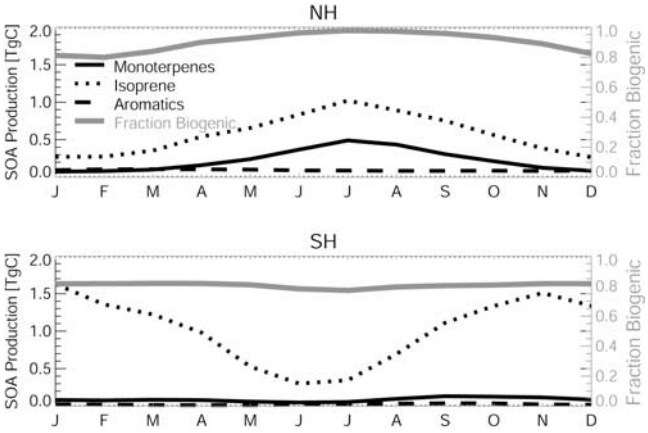

Figure 5. Seasonal cycle of simulated SOA production for the year 2000 in the (top) Northern and(bottom) Southern Hemisphere for each precursor. The fraction of SOA produced from biogenic precursors is shown with the scale on the right axis.

[2008] report SOA production from aromatic, monoterpene, and isoprene of 3.5 Tg a^{-1}, 8.2 Tg a^{-1} and 13.2 Tg a^{-1}. Upon accounting for differences in precursor emissions employed in these simulations, we find that while SOA production and the resulting burden from aromatic sources simulated here agrees well with the estimates of *Henze et al.* [2008], production from biogenic sources appears to be more than a factor of two more efficient in our simulation. We attribute this to enhanced POA emissions, the tropical tropospheric cold bias of CCSM3 [*Collins et al.*, 2006b] and differences in convection. Similar differences exist among previous model simulations reported in the literature, for example the biogenic SOA production (nonisoprene only) reported by *Tsigaridis and Kanakidou* [2003] is about half of *Henze et al.* [2008], who use lower emissions. In what follows, we focus on relative differences in SOA, thereby limiting the importance of these differences on our conclusions. SOA makes up 39% of the total OC aerosol burden and 35% of the source of OC (primary emission + SOA production) in our simulation.

3.2. Sensitivity of SOA to Future Anthropogenic Emissions

[29] The changes in SOA concentrations resulting from climate, emissions, and land use change (Table 1) in the year 2100 are shown in Figures 6 and 7 (note that scales for all the figures are set to half of their present-day concentration scales in Figures 3 and 4). These results will be discussed separately here in sections 3.2–3.5, and summarized in Figure 9 and section 4. The differences between future and present-day simulations shown here are all significant when tested against the effects of interannual climate variability (from the 10-year future simulations). In particular, we note that the interannual variability in zonal mean SOA concentrations is 0.01 μg C m^{-3} or less throughout the troposphere, values which appear as white or "no difference" on Figure 7.

[30] Figures 6 and 7 show the changes in annual mean surface and zonal SOA concentrations induced by 2100 A1B anthropogenic emissions but maintaining present-day biogenic emissions and climate (2100A). The concentration of SOA produced from aromatic precursors changes by up to a factor of two over the continental regions, as a result of the projected change in aromatic emissions (Figure 1). The exception to this behavior is Japan where, despite a projected decrease in aromatic emissions, aromatic SOA concentrations are projected to rise because of the anticipated increases in outflow from China. POA emissions are projected to increase globally by 60% (Figure 1), and yet this increase alone (2100Ao-2000) causes the global anthropogenic SOA burden to increase by less than 5% with a maximum increase of 15% in surface anthropogenic SOA concentrations over Asia. Anthropogenic semivolatiles are efficiently converted to aerosol near the source and this conversion is not appreciably accelerated by the addition of condensational mass in the form of POA emission. In the regions where aromatic emissions are projected to decrease (North America and Europe), this decline dominates the effect of POA increases, leading to overall reductions in anthropogenic SOA. Hydroxyl radical concentrations decrease in the Northern Hemisphere by 5–20%, largely the result of decreases in nitrogen oxide emissions projected over North America and Europe and increased CO emissions in Asia, consistent with the oxidant sensitivities examined by *Grenfell et al.* [2003]. Slower aromatic oxidation by OH delays subsequent SOA formation, thus producing longer-lived SOA aloft. However, the increase in SOA burden from increased lifetime is minor compared to the direct effect of emissions changes. The global burden of aromatic SOA increases by 53% in 2100 compared to 2000.

[31] Future anthropogenic emissions indirectly increase the global burden of SOA from monoterpene sources by 10% as a result of rising POA emissions. *Liao et al.* [2006] predict a 31% increase for a greater than twofold increase in POA emissions (here emissions increase by 60%). Biogenic SOA formation is generally not geographically coincident with anthropogenic emissions, and is therefore far more sensitive to the available condensational mass than anthropogenic SOA. Additionally, the nonlinearity of SOA partitioning implies that changes in aromatic SOA

Table 4. Annual Total Net Tropospheric SOA Production From Each Precursor (Surface to 200 hPa)[a]

Species	2000	2100A	2100B	2100C	2100ABC	2100L[b]
SOA (monoterpenes)	3.7	4.1 (+12%)	4.6 (+23%)	3.7 (+1%)	4.9 (+31%)	(−11%)
SOA (isoprene)	19.2	20.3 (+6%)	24.4 (+27%)	19.3(+1%)	23.4 (+22%)	(−15%)
SOA (aromatics)	1.4	2.0 (+42%)	1.4 (+1%)	1.4 (+1%)	2.0 (+41%)	(0%)
Total SOA	24.3	26.5 (+9%)	30.5 (+26%)	24.4 (+1%)	30.2 (+24%)	(−13%)

[a]Unit is Tg C a^{-1} (percent differences from 2000 in brackets). Totals may not add as numbers are rounded independently.
[b]Changes in SOA due to anthropogenic land use change require the use of fixed isoprene emission factors, therefore percentage changes from the 2000L simulation are shown for comparison.

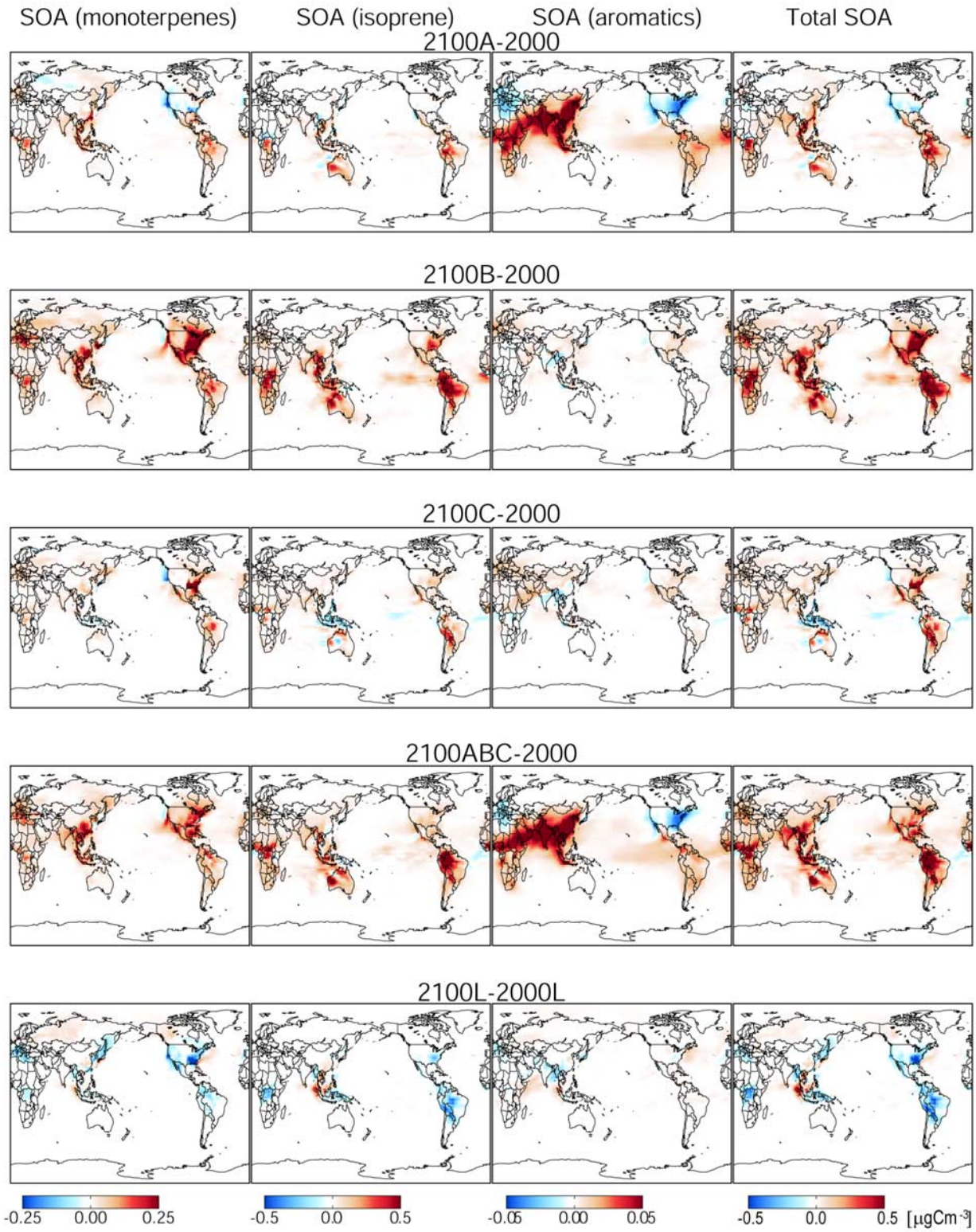

Figure 6. Annual global change in surface SOA concentrations for each SOA component for 2100 from the base case of 2000 (Figure 3). Simulations are performed with future anthropogenic emissions (2100A), future biogenic emissions (2100B), and future climate (2100C). The changes from the present day with both future emissions and climate (2100ABC), representing the combined effect, are also shown. The fifth row shows the effect of future anthropogenic land use change (2100L). Color scales are saturated at minimum and maximum value and are set to half the maximum values of Figure 3.

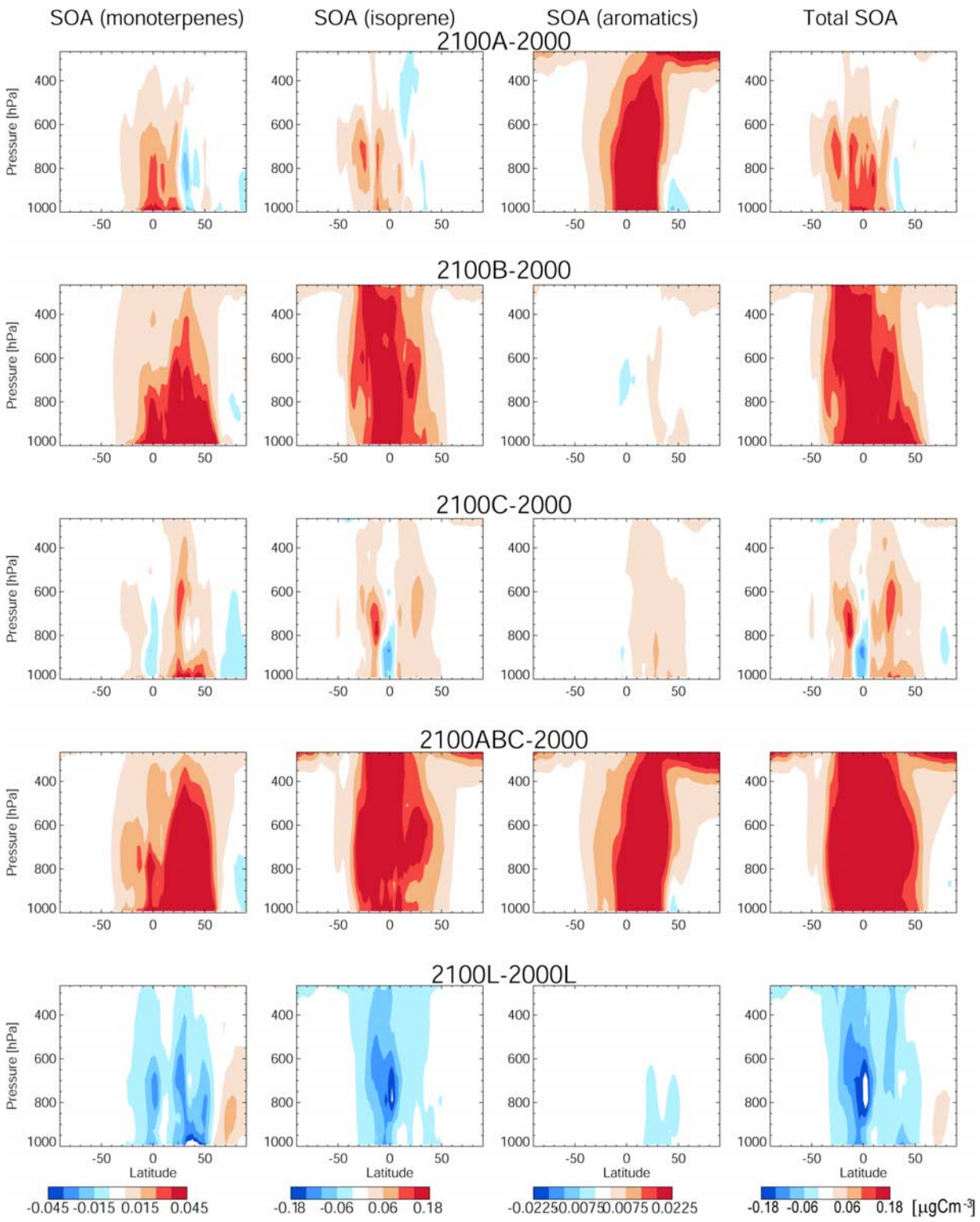

Figure 7. Annual global change in zonal mean SOA concentrations for each SOA component for 2100 from the base case of 2000 (Figure 4). Simulations are performed with future anthropogenic emissions (2100A), future biogenic emissions (2100B) and future climate (2100C). The changes from the present day with both future emissions and climate (2100ABC), representing the combined effect, are also shown. The fifth row shows the effect of future anthropogenic land use change (2100L). Color scales are saturated at minimum and maximum values and are set to approximately half the maximum values of Figure 4.

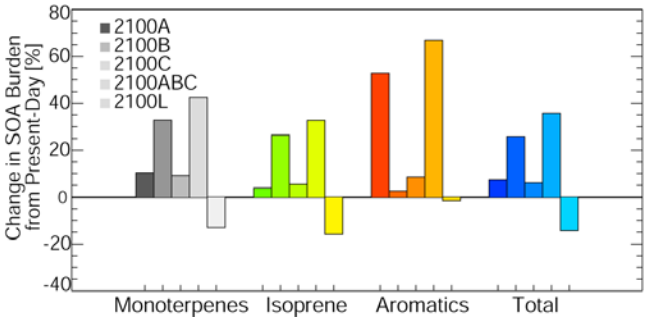

Figure 8. Percentage change in simulated 2100 global mean SOA burden from present-day (2000) baseline. SOA from monoterpenes (grey), isoprene (yellow) and aromatic (orange) precursors are shown individually with percentage change in total SOA shown in blue. Simulations are performed with future anthropogenic emissions (2100A), future biogenic emissions (2100B) future climate (2100C), and future land use (2100L, relative to 2000L, see Table 1). The changes from the present day with both future emissions and climate (2100ABC), representing the combined effect, are also shown.

concentrations feed back onto SOA formation, notably leading to modest reductions in SOA from monoterpenes over North America (where aromatic emissions decrease by −61%).

[32] The effect of anthropogenic emissions on the global burden of SOA from isoprene oxidation is small (4% increase). Aerosol formation is modestly enhanced by global increases in POA emissions (8% increase). However, only products of isoprene reaction with OH lead to aerosol formation here, therefore the tropical increases in O_3 and NO_3 induced by future global anthropogenic emissions [*Grenfell et al.*, 2003; *Brasseur et al.*, 2006] deplete the pool of SOA precursor available, offsetting some of the SOA increases from increased POA emissions.

[33] Overall, anthropogenic emission changes projected by the A1B scenario (27% increase in aromatics and 60% increase in POA) lead to a 7% increase in the total SOA burden in 2100. This includes increases for both biogenic and anthropogenic SOA.

[34] Key differences in the socioeconomic assumptions of the A1B and A2 IPCC emission scenarios translate to either reduction or growth in aromatic emissions for some important source regions (North America and Europe). Should these regions follow an increasing emission pathway (such as the A2 scenario), anthropogenic SOA increases for 2100 would be significantly higher (+139%) than that shown here with the A1B (Figure 6).

3.3. Sensitivity of SOA to Future Biogenic Emissions

[35] The increase in global biogenic emissions (22%, see section 2.3) in 2100 leads to a 26% increase in the global annual mean SOA burden when climate and anthropogenic emissions are maintained at the present day (2100B). Outside of the tropics, the majority of this increase in burden takes place in local summer. Changes in biogenic SOA concentrations (Figure 6) coincide directly with the patterns of emission changes seen in Figure 2. Formation of biogenic SOA is enhanced not only by precursor emission increases, but also as a result of additional aerosol partitioning on newly formed SOA. Global annual mean surface concentrations of SOA from isoprene increase by 30%, most importantly over the southeastern United States and South America. Relative increases in SOA from monoterpene oxidation are even greater, primarily because of enhanced ozonolysis, with a 41% global increase in surface concentrations. Increased isoprene concentrations simulated in 2100 increase surface O_3, consistent with the 10–20 ppb increase reported by *Sanderson et al.* [2003] for a comparable isoprene emission increase. SOA formation from the ozonolysis of isoprene is small compared to reaction with OH [*Kleindienst et al.*, 2007], and not included in these simulations. However, we note that inclusion of this formation pathway would lead to a further increase in SOA from isoprene in response to future biogenic emission increases. Figure 7 shows that predicted SOA concentrations are elevated throughout the depth of the troposphere. Future biogenic emissions amplify mean surface concentrations of anthropogenic SOA by 5%. Aerosol partitioning is enhanced by the additional biogenic SOA; however, increases in isoprene emissions deplete the OH available for oxidation, leading to some compensating decreases (5–20%) in aromatic and monoterpene SOA formation in localized regions.

3.4. Sensitivity of SOA to Future Climate

[36] Global SOA production is essentially constant under a climate-change-only scenario (2100C), with the exception of the biogenic emissions temperature response (which we categorize as an "emissions" change) detailed in section 3.3. However, changes in aerosol lifetime in a future climate result in a 6% increase in global mean SOA burden (Figure 8). Regional surface concentrations do not change by more than 25%. The climate response of SOA includes changes in aerosol partitioning, as well as oxidation and removal rates (via precipitation). In some regions these effects neutralize one another.

[37] The warming troposphere implies a 5–15% decrease in aerosol partitioning, as implemented by the Clausius-Clayperon adjustment to the partitioning coefficients of equation (2). This effect would be largest in the cold upper troposphere, a region of limited SOA formation. However, decreased aerosol partitioning is buffered by the transport of evaporated semivolatiles which allows for reformation of aerosol downwind. Our results predict less than 1% change in SOA production under future climate (Table 4). A lower enthalpy of vaporization for the aromatic SOA species (see section 2.1) would act to further reduce the minimal sensitivity to temperature seen here. *Tsigaridis and Kanakidou* [2007] predict an 11% decrease in SOA burden in response to a fixed temperature increase of 1–2°K; the SOA burden simulated here with a more sophisticated description of tropospheric warming appears to be less sensitive to changes in aerosol partitioning, although we do not explicitly separate this effect.

[38] Hydroxyl radical concentrations increase under climate-change-only scenarios as a result of both enhanced tropospheric water vapor and increases in nitrogen oxide (NO_x) emissions from lightning in the upper troposphere [*Grenfell et al.*, 2003; *Brasseur et al.*, 2006]. Global mean tropospheric OH concentrations simulated here increase by

9%. A 27% increase in lightning NOx emissions enhances O_3, a source of OH, in the tropical upper troposphere. The warmer 2100 atmosphere holds more water vapor throughout the atmosphere than the present day, by more than 50% in the tropical upper troposphere (annual mean). This water vapor also enhances OH formation, speeding up oxidation in the tropical troposphere. In particular, more isoprene is oxidized over the continents, reducing formation downwind (Figure 6), consistent with the effect predicted by *Tsigaridis and Kanakidou* [2007]. Ozone concentrations decrease by 5–10% in the extratropics as a result of more rapid loss due to elevated water vapor [*Brasseur et al.*, 2006], thereby delaying SOA formation from monoterpenes.

[39] Precipitation rates in the CCSM 2100 A1B climate increase in the tropics and decrease in the subtropics, particularly over the oceans [*Meehl et al.*, 2006]. The increased removal in the tropical outflow region contributes to the reductions of isoprene SOA over this region (Figure 6). Aerosol lifetimes increase with the drier climate, and surface concentrations of SOA increase by 5–25% as a result.

[40] Overall, production of SOA in the future climate, in the absence of other changes, is predicted to change by less than 1% but with small mean increases in atmospheric lifetime (10–16 h), the global mean burden increases by 6%. This result is consistent across both biogenic and anthropogenic SOA classes.

3.5. Sensitivity of SOA to Projected Land Use Change

[41] Changes in the global vegetation distribution, either induced by human activity or in response to climate change, represent an important and highly uncertain control on natural emissions to the troposphere. Historical land cover data have been used to explore the importance of this effect [*Purves et al.*, 2004; *Tao and Jain*, 2005]. However, prediction of natural vegetation changes rely on dynamic vegetation models which exhibit a large range of biospheric responses to CO_2 and climate change [*Cramer et al.*, 2001]. One study indicates that foliar expansion and ecosystem modification leads to an 87% increase in isoprene emissions above the baseline increase predicted for a 2100 climate with fixed vegetation [*Lathière et al.*, 2005]. This is largely the result of expansion of the boreal and temperate forests of North America and Eurasia. Another study finds that the dieback of the Amazonian forest predicted by 2100 may decrease isoprene emissions [*Sanderson et al.*, 2003]. These studies focus on changes in vegetation distribution (i.e., PFT fractions), but do not consider changes in species composition. We focus here on predicted anthropogenic land use change rather than natural vegetation redistribution, but recognize that natural vegetation could be the dominant, if highly uncertain, control on future emission.

[42] We employ the land cover change predictions of J. J. Feddema et al. (A global land cover dataset for use in transient climate simulations, submitted to *Journal of Applied Meteorology and Climatology*, 2007) which are based on the present-day vegetation distribution of *Lawrence and Chase* [2007]. Changes to croplands and grazing areas simulated by the IMAGE 2.2 model for the IPCC A2 scenario are adapted to the plant functional type distribution used in CLM. Of the IPCC scenarios characterized by different socioeconomic assumptions, the A2 scenario predicts the largest human-induced change in land cover. We use it here as the largest predicted change in land cover, which can be compared to the effects of emissions and climate on global SOA as examined in sections 3.2–3.4. This scenario predicts the expansion of croplands and grasses (low BVOC emitters) at the expense of broadleaf forest (high BVOC emitters) in 2100. The A1B scenario predicts a more modest perturbation to land cover, with similar geographical distribution.

[43] The current MEGAN2 emission scheme includes species-specific basal emission rates for each grid box, however the geographical migration of plant species within a plant functional type as a consequence of climate change has not been investigated. Therefore, to simulate the response of BVOC emissions to changes in vegetation distribution we revert to fixed emission factors for each plant functional type [*Guenther et al.*, 1995] for isoprene (2000L). As previously found [*Lathière et al.*, 2005], fixed emission factors result in lower baseline isoprene emissions (here 359 Tg C a^{-1}). All changes in SOA with the 2100 vegetation distribution (2100L) are reported with respect to this alternate baseline simulation.

[44] Figure 2 shows the pattern of predicted change in BVOC emissions for the year 2100 under the A2 land use change scenario. Global isoprene and monoterpene emissions decrease by 15% and 10%, respectively. Cropland expansion in South America, sub-Saharan Africa, China, and the United States reduce BVOC emissions from these regions in the year 2100. Small increases in fineleaf tree cover also enhance monoterpene emissions at high latitudes. A sensitivity study by [*Lathière et al.*, 2006] found that a complete tropical deforestation scenario implied a 29% global decrease in isoprene emissions, consistent with the results shown here.

[45] Projected agricultural expansion and increased urbanization by 2100 leads to an overall reduction in the global annual mean SOA burden by 14%, when climate and emissions are fixed at present-day conditions (2100L). Biogenic SOA production drops by 14% globally and surface concentrations decrease by 5–25%; the largest relative differences are found over the southeastern United States and South America (Figure 6). The reduction in aromatic SOA burden is slight, with regional decreases less than 10%. The global reduction in biogenic SOA due to an A2 land use change scenario compensates for more than half of the temperature-driven increase in biogenic SOA projected in an A1B scenario (section 3.3).

4. Discussion and Conclusions

[46] Figure 8 synthesizes the SOA sensitivities reported in section 3. The integrated effect of future climate and emissions (IPCC A1B) simulated here is a 36% increase in global SOA burden and a 24% increase in global SOA production by 2100. Our results indicate that this increase may be tempered (14% decrease in burden) by the expansion of croplands projected for 2100 (section 3.4). This may be further modulated by natural vegetation responses including the expansion of the boreal forests [*Lathière et al.*, 2005] and the dieback of Amazonian forests [*Sanderson et al.*, 2003], which we do not consider here. The future

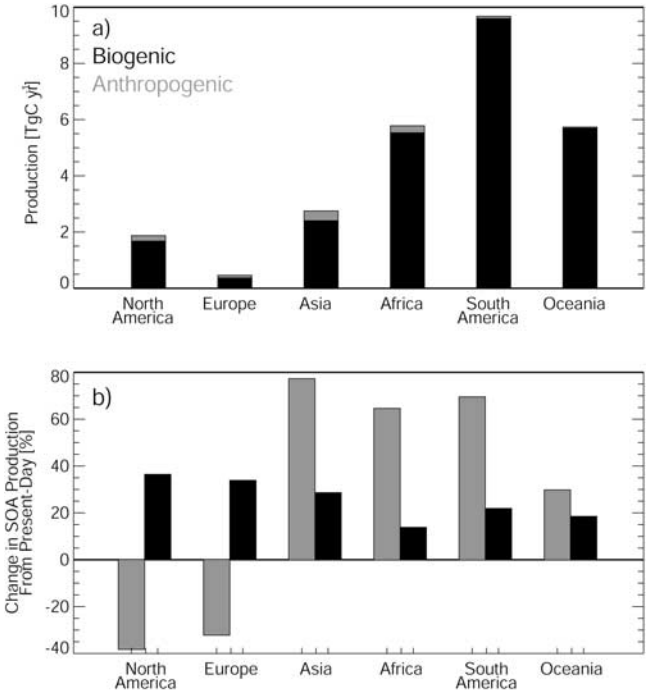

Figure 9. Annual total simulated SOA production by region (surface-200 hPa) (a) in the present day (2000) and (b) percentage change in 2100 from 2000 with both emission and climate changes according to IPCC A1B scenario (2100ABC). SOA from biogenic precursors (monoterpenes + isoprene) are shown as black bars and anthropogenic (aromatic) SOA are shown as grey bars. Regions include the continent and immediate downwind oceanic outflow region.

distribution of vegetation is a potentially large, and highly uncertain, control on global SOA concentrations.

[47] Future projected increases in the global SOA burden are largely dictated by emission increases with anthropogenic emissions increasing mainly in Asia and the Southern Hemisphere and BVOC emissions increasing mainly in response to temperature, consistent with the results of *Tsigaridis and Kanakidou* [2007]. Emissions of SOA precursors not included here (sesquiterpenes and long-chain oxygenated VOCs) may be even more temperature sensitive [*Helmig et al.*, 2007]. The response of SOA to emissions increases is primarily a first-order effect, with feedbacks on oxidant concentrations and condensation mass of secondary importance. Biogenic SOA formation is also strongly sensitive to increases in POA emissions. Therefore the efficiency of inorganic aerosols as condensation surfaces for SOA, which has not been explored in the laboratory or accounted for here, remains a critical open question. *Tsigaridis and Kanakidou* [2003] suggest that this effect could be large with a simulated 87% increase in present-day SOA production when including condensation on sulfate and ammonium aerosols. Condensation of SOA on sulfate would enhance simulated present-day aerosol partitioning, however the importance of this effect would diminish over time if global sulfur emissions follow projected decreases (−62% in 2100 for A1B [*Horowitz*, 2006]), thus reducing the difference between future and present-day SOA. A box model study suggests that SOA formation is very sensitive to interactions with water [*Pun and Seigneur*, 2007]. Accounting for water from hygroscopic aerosol growth in condensational mass would provide an additional climate control on SOA formation. Guidance from laboratory studies is required on the composition and relative efficacy of absorbing aerosol mass. Anthropogenic SOA formation is less sensitive to increases in POA emissions, suggesting that high-efficiency conversion of semivolatiles to aerosol near the source is achieved with present-day POA emissions.

[48] Changes in oxidant concentrations and temperature predicted in the 2100 A1B climate by the CAM3 model, taken together, do not significantly modify global SOA production. However, changes in precipitation lengthen the SOA lifetime and lead to a 6% increase in predicted SOA burden. The decrease in aerosol partitioning due to a warmer climate is not a dominant factor in the SOA budget changes predicted over a century, therefore the use of a single enthalpy of vaporization for partitioning coefficient adjustments is not a primary uncertainty in the changes predicted by this study. The largest relevant uncertainty in these climate predictions are the changes in the hydrological cycle [*IPCC*, 2007] which controls the lifetime of SOA in the atmosphere.

[49] Figure 9a shows the regional production of SOA. Tropospheric production is summed over each continent, including the immediate outflow region. South America is the largest source region in the year 2000, with a negligible contribution from anthropogenic sources. Global SOA production is dominated by biogenic sources in the Southern Hemisphere in this simulation. The majority of ambient observations of OC aerosol have been reported in the Northern Hemisphere, including those reporting a discrepancy between current models and observations [*Volkamer et al.*, 2006, and references therein]. In addition, the algorithms developed to capture the environmental variation of biogenic emissions have relied, necessarily, in large part on measurements in the Northern Hemisphere [*Guenther et al.*, 2006]. There is a critical need for comprehensive aerosol and biogenic emission measurements throughout the Southern Hemisphere to test existing models. Projected SOA production in 2100 is still dominated by South America, however we show in Figure 9b that Asia experiences the largest relative growth in SOA production (78% anthropogenic SOA, 29% biogenic SOA). The relative importance of Asia as a global source of SOA depends critically on the balance between anthropogenic and biogenic sources. Several studies have suggested that anthropogenic SOA is underestimated by current models [*de Gouw et al.*, 2005; *Sullivan et al.*, 2006; *Volkamer et al.*, 2006], which implies that the large increases in anthropogenic aromatic emissions projected for Asia, may have important implications for climate forcing and the degradation of air quality locally in Asia and downwind over North America.

[50] These simulations show that even under the A1B scenario the anthropogenic SOA burden is more sensitive (67% increase) to predicted future changes than biogenic SOA (35% increase). Our results predict that less than 10% of global SOA in 2100 is anthropogenic in origin, however expansion of croplands, dieback of the Amazon, model underestimate of anthropogenic SOA and/or faster anthro-

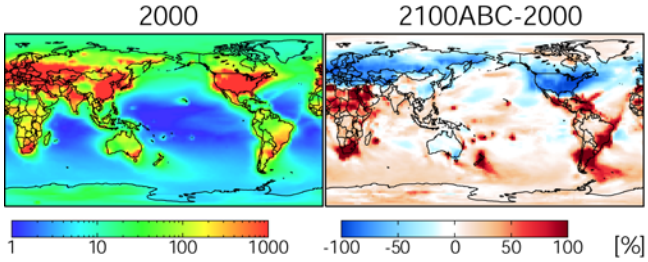

Figure 10. (left) Surface ratio of NO/HO_2 concentrations simulated for the year 2000 and (right) the difference between 2100ABC (with both climate and emissions change, see Table 1) and 2000. Color scales are saturated at respective values.

pogenic emission increases would all increase the fraction of anthropogenic SOA in 2100 beyond these levels.

[51] Both isoprene [*Kroll et al.*, 2005] and aromatics [*Ng et al.*, 2007a] produce SOA more efficiently under low nitrogen oxide (NO_x) concentrations; the inverse may be true for sesquiterpenes [*Ng et al.*, 2007b]. This represents an anthropogenic control on SOA formation. *Kroll et al.* [2006] suggest that the NO/HO_2 ratio serves as a diagnostic of SOA formation efficiency, reflecting the importance of peroxy radicals in SOA product formation. Figure 10 shows the predicted change in surface NO/HO_2 ratio in 2100 (A1B). NO_x emission reductions in Europe and North America would lead to more efficient SOA formation (isoprene and aromatic SOA); on the other hand, NOx emission increases throughout much of the Southern Hemisphere and tropics would lead to less efficient formation. Globally, NO_x emissions are predicted to increase by 17% by 2100 under the A1B scenario (Table 2). Characterizing laboratory SOA yields as a function of NO/HO_2 is vital for predicting how SOA formation will respond to changes in anthropogenic emissions, particularly in urban environments.

[52] Observations indicate that current estimates of global SOA formation are underestimated by up to two orders of magnitude [*Volkamer et al.*, 2006]. Our results suggests that SOA will become an increasingly important fraction of the global aerosol burden, affecting both climate and air quality. In particular, anthropogenic control of SOA formation, both direct and indirect, may be an important regulator on the Earth's climate. *Andreae et al.* [2005] suggest that anticipated reductions in sulfate will accelerate greenhouse gas induced warming in the coming century, however the upward trend in secondary organic aerosol concentrations predicted here may compensate for this effect. The present-day SOA burden simulated here (0.59 Tg C), is comparable to estimates of the global sulfate burden (0.5–0.7 Tg S [*Koch et al.*, 1999; *Barth et al.*, 2000; *Takemura et al.*, 2000]). Sulfur emissions are predicted to decline by more than 50% by 2100 (A1B) [*Horowitz*, 2006], compared with a 36% increase in SOA predicted here. In addition, large increases in primary organic aerosol emissions (present-day burden of 1.2 Tg [*Chung and Seinfeld*, 2002]) are also anticipated in the A1B scenario. The relative importance of OC aerosol-induced cooling depends critically on the total burden in the atmosphere and the highly uncertain optical properties of this aerosol (including consideration of hygroscopicity and noncarbon composition). Therefore the role of predicted SOA increases in counteracting the climatic effects of predicted decreases in sulfate aerosol could be large, and requires further investigation.

[53] This study highlights how SOA, as simulated in current global models, will respond to a subset of chemistry-climate-emissions drivers which almost certainly do not describe the complete sensitivities of this complex system. Further experimental investigation of SOA formation efficiency, spanning the range of ambient conditions, is essential to predicting how SOA will respond and contribute to climate change.

[54] **Acknowledgments.** The use of the computing time for the model experiments was supplied through the National Center for Atmospheric Research, Community Climate System Model (CCSM) Chemistry-Climate Group, which is sponsored by the National Science Foundation. We acknowledge the RETRO project for providing aromatic emission inventories. We thank Gary Strand (NCAR) for providing archived SST fields and Sam Levis (NCAR) for assistance with CLM3. C.L.H. gratefully acknowledges support by the NOAA global climate change postdoctoral fellowship, administered by the University Corporation for Atmospheric Research.

References

Alessio, G. A., M. De Lillis, M. Fanelli, P. Pinelli, and F. Loreto (2004), Direct and indirect impacts of fire on isoprenoid emissions from Mediterranean vegetation, *Functional Ecol.*, *18*(3), 357–364.

Andreae, M. O., C. D. Jones, and P. M. Cox (2005), Strong present-day aerosol cooling implies a hot future, *Nature*, *435*(7046), 1187–1190.

Arneth, A., et al. (2007), Process-based estimates of terrestrial ecosystem isoprene emissions: incorporating the effects of a direct CO2-isoprene interaction, *Atmos. Chem. Phys.*, *7*, 31–53.

Balkanski, Y. J., D. J. Jacob, G. M. Gardner, W. C. Graustein, and K. K. Turekian (1993), Transport and residence times of tropospheric aerosols inferred from a global 3-dimensional simultion of Pb-210, *J. Geophys. Res.*, *98*(D11), 20,573–20,586.

Barth, M. C., P. J. Rasch, J. T. Kiehl, C. M. Benkovitz, and S. E. Schwartz (2000), Sulfur chemistry in the National Center for Atmospheric Research Community Climate Model: Description, evaluation, features, and sensitivity to aqueous chemistry, *J. Geophys. Res.*, *105*(D1), 1387–1415.

Bonan, G. B., S. Levis, L. Kergoat, and K. W. Oleson (2002), Landscapes as patches of plant functional types: An integrating concept for climate and ecosystem models, *Global Biogeochem. Cycles*, *16*(2), 1021, doi:10.1029/2000GB001360.

Brasseur, G. P., D. A. Hauglustaine, S. Walters, P. J. Rasch, J. F. Muller, C. Granier, and X. X. Tie (1998), MOZART, a global chemical transport model for ozone and related chemical tracers: 1. Model description, *J. Geophys. Res.*, *103*(D21), 28,265–28,289.

Brasseur, G. P., et al. (2006), Impact of climate change on the future chemical composition of the global troposphere, *J. Clim.*, *19*(16), 3932–3951.

Carlton, A. G., B. J. Turpin, H.-J. Lim, K. E. Altieri, and S. Seitzinger (2006), Link between isoprene and secondary organic aerosol (SOA): Pyruvic acid oxidation yields low volatility organic acids in clouds, *Geophys. Res. Lett.*, *33*, L06822, doi:10.1029/2005GL025374.

Chen, W.-T., H. Liao, and J. H. Seinfeld (2007), Future climate impacts of direct radiative forcing of anthropogenic aerosols, tropospheric ozone, and long-lived greenhouse gases, *J. Geophys. Res.*, *112*, D14209, doi:10.1029/2006JD008051.

Chung, S. H., and J. H. Seinfeld (2002), Global distribution and climate forcing of carbonaceous aerosols, *J. Geophys. Res.*, *107*(D19), 4407, doi:10.1029/2001JD001397.

Collins, W. D., et al. (2006a), The Community Climate System Model version 3 (CCSM3), *J. Clim.*, *19*(11), 2122–2143.

Collins, W. D., et al. (2006b), The formulation and atmospheric simulation of the Community Atmosphere Model version 3 (CAM3), *J. Clim.*, *19*(11), 2144–2161.

Cooke, W. F., C. Liousse, H. Cachier, and J. Feichter (1999), Construction of a 1° × 1° fossil fuel emission data set for carbonaceous aerosol and implementation and radiative impact in the ECHAM4 model, *J. Geophys. Res.*, *104*(D18), 22,137–22,162.

Cramer, W., et al. (2001), Global response of terrestrial ecosystem structure and function to CO2 and climate change: Results from six dynamic global vegetation models, *Global Change Biol.*, *7*(4), 357–373.

de Gouw, J. A., et al. (2005), Budget of organic carbon in a polluted atmosphere: Results from the New England Air Quality Study in 2002, *J. Geophys. Res.*, *110*, D16305, doi:10.1029/2004JD005623.

Dickinson, R. E., et al. (2006), The Community Land Model and its climate statistics as a component of the Community Climate System Model, *J. Clim.*, *19*(11), 2302–2324.

Drake, B. G., M. A. GonzalezMeler, and S. P. Long (1997), More efficient plants: A consequence of rising atmospheric CO_2?, *Annu. Rev. Plant Phys. Plant Mol. Biol.*, *48*, 609–639.

Gao, S., et al. (2004), Particle phase acidity and oligomer formation in secondary organic aerosol, *Environ. Sci. Technol.*, *38*(24), 6582–6589.

Ginoux, P., L. W. Horowitz, V. Ramaswamy, I. V. Geogdzhayev, B. N. Holben, G. Stenchikov, and X. Tie (2006), Evaluation of aerosol distribution and optical depth in the Geophysical Fluid Dynamics Laboratory coupled model CM2.1 for present climate, *J. Geophys. Res.*, *111*, D22210, doi:10.1029/2005JD006707.

Giorgi, F., and W. L. Chameides (1985), The rainout parameterization in a photochemical model, *J. Geophys. Res.*, *90*(D5), 7872–7880.

Goldstein, A. H., and I. E. Galbally (2007), Known and unexplored organic constituents in the earth's atmosphere, *Environ. Sci. Technol.*, *41*(5), 1514–1521.

Grenfell, J. L., D. T. Shindell, and V. Grewe (2003), Sensitivity studies of oxidative changes in the troposphere in 2100 using the GISS GCM, *Atmos. Chem. Phys.*, *3*, 1267–1283.

Grewe, V., M. Dameris, R. Hein, R. Sausen, and B. Steil (2001), Future changes of the atmospheric composition and the impact of climate change, *Tellus, Ser. B*, *53*(2), 103–121.

Griffin, R. J., D. R. Cocker, R. C. Flagan, and J. H. Seinfeld (1999), Organic aerosol formation from the oxidation of biogenic hydrocarbons, *J. Geophys. Res.*, *104*(D3), 3555–3567.

Guenther, A., et al. (1995), A global model of natural volatile organic compound emissions, *J. Geophys. Res.*, *100*(D5), 8873–8892.

Guenther, A., T. Karl, P. Harley, C. Wiedinmyer, P. I. Palmer, and C. Geron (2006), Estimates of global terrestrial isoprene emissions using MEGAN (Model of Emissions of Gases and Aerosols from Nature), *Atmos. Chem. Phys.*, *6*, 3181–3210.

Hao, W. M., and M. H. Liu (1994), Spatial and temporal distribution of tropical biomass burning, *Global Biogeochem. Cycles*, *8*(4), 495–503.

Harley, P. C., M. E. Litvak, T. D. Sharkey, and R. K. Monson (1994), Isoprene emission from velvet bean leaves—Interactions among nitrogen availability, growth photon flux density, and leaf development, *Plant Physiol.*, *105*(1), 279–285.

Heald, C. L., D. J. Jacob, R. J. Park, L. M. Russell, B. J. Huebert, J. H. Seinfeld, H. Liao, and R. J. Weber (2005), A large organic aerosol source in the free troposphere missing from current models, *Geophys. Res. Lett.*, *32*, L18809, doi:10.1029/2005GL023831.

Helmig, D., et al. (2007), Sesquiterpene emissions from pine trees - Identifications, emission rates and flux estimates for the contiguous United States, *Environ. Sci. Technol.*, *41*(5), 1545–1553.

Henze, D. K., and J. H. Seinfeld (2006), Global secondary organic aerosol from isoprene oxidation, *Geophys. Res. Lett.*, *33*, L09812, doi:10.1029/2006GL025976.

Henze, D. K., J. H. Seinfeld, N. L. Ng, J. H. Kroll, M. Fu, and C. L. Heald (2008), Global modeling of secondary organic aerosol formation from aromatic hydrocarbons: High-vs-low-yield pathways, *Atmos. Chem. Phys.*, in press.

Horowitz, L. W. (2006), Past, present, and future concentrations of tropospheric ozone and aerosols: Methodology, ozone evaluation, and sensitivity to aerosol wet removal, *J. Geophys. Res.*, *111*, D22211, doi:10.1029/2005JD006937.

Horowitz, L. W., et al. (2003), A global simulation of tropospheric ozone and related tracers: Description and evaluation of MOZART, version 2, *J. Geophys. Res.*, *108*(D24), 4784, doi:10.1029/2002JD002853.

Intergovernmental Panel on Climate Change (2001), *Climate Change 2001: The Scientific Basis*, 881 pp., Cambridge Univ. Press, Cambridge, U. K.

Intergovernmental Panel on Climate Change (2007), *Climate Change 2007: The Physical Science Basis*, 996 pp., Cambridge Univ. Press, Cambridge, U. K.

Jang, M. S., and R. M. Kamens (2001), Characterization of secondary aerosol from the photooxidation of toluene in the presence of NOx and 1-propene, *Environ. Sci. Technol.*, *35*(18), 3626–3639.

Johnson, D., M. E. Jenkin, K. Wirtz, and M. Martin-Reviejo (2005), Simulating the formation of secondary organic aerosol from the photooxidation of aromatic hydrocarbons, *Environ. Chem.*, *2*(1), 35–48.

Johnson, D., et al. (2006), Simulating regional scale secondary organic aerosol formation during the TORCH 2003 campaign in the southern UK, *Atmos. Chem. Phys.*, *6*, 403–418.

Kalberer, M., et al. (2004), Identification of polymers as major components of atmospheric organic aerosols, *Science*, *303*(5664), 1659–1662.

Kanakidou, M., et al. (2005), Organic aerosol and global climate modelling: A review, *Atmos. Chem. Phys.*, *5*, 1053–1123.

Kiehl, J. T., C. A. Shields, J. J. Hack, and W. D. Collins (2006), The climate sensitivity of the Community Climate System Model version 3 (CCSM3), *J. Clim.*, *19*(11), 2584–2596.

Kinnison, D. E., et al. (2007), Sensitivity of chemical tracers to meteorological parameters in the MOZART-3 chemical transport model, *J. Geophys. Res.*, *112*, D20302, doi:10.1029/2006JD007879.

Kleindienst, T. E., T. S. Conver, C. D. McIver, and E. O. Edney (2004), Determination of secondary organic aerosol products from the photooxidation of toluene and their implications in ambient PM2.5, *J. Atmos. Chem.*, *47*(1), 79–100.

Kleindienst, T. E., M. Lewandowski, J. H. Offenberg, M. Jaoui, and E. O. Edney (2007), Ozone-isoprene reaction: Re-examination of the formation of secondary organic aerosol, *Geophys. Res. Lett.*, *34*, L01805, doi:10.1029/2006GL027485.

Koch, D., D. Jacob, I. Tegen, D. Rind, and M. Chin (1999), Tropospheric sulfur simulation and sulfate direct radiative forcing in the Goddard Institute for Space Studies general circulation model, *J. Geophys. Res.*, *104*(D19), 23,799–23,822.

Korner, C. (2000), Biosphere responses to CO_2 enrichment, *Ecol. Appl.*, *10*(6), 1590–1619.

Kroll, J. H., N. L. Ng, S. M. Murphy, R. C. Flagan, and J. H. Seinfeld (2005), Secondary organic aerosol formation from isoprene photooxidation under high-NO_x conditions, *Geophys. Res. Lett.*, *32*, L18808, doi:10.1029/2005GL023637.

Kroll, J. H., N. L. Ng, S. M. Murphy, R. C. Flagan, and J. H. Seinfeld (2006), Secondary organic aerosol formation from isoprene photooxidation, *Environ. Sci. Technol.*, *40*(6), 1869–1877.

Lack, D. A., X. X. Tie, N. D. Bofinger, A. N. Wiegand, and S. Madronich (2004), Seasonal variability of secondary organic aerosol: A global modeling study, *J. Geophys. Res.*, *109*, D03203, doi:10.1029/2003JD003418.

Lamarque, J.-F., J. T. Kiehl, P. G. Hess, W. D. Collins, L. K. Emmons, P. Ginoux, C. Luo, and X. X. Tie (2005), Response of a coupled chemistry-climate model to changes in aerosol emissions: Global impact on the hydrological cycle and the tropospheric burdens of OH, ozone, and NO_x, *Geophys. Res. Lett.*, *32*, L16809, doi:10.1029/2005GL023419.

Lathière, J., D. A. Hauglustaine, N. De Noblet-Ducoudré, G. Krinner, and G. A. Folberth (2005), Past and future changes in biogenic volatile organic compound emissions simulated with a global dynamic vegetation model, *Geophys. Res. Lett.*, *32*, L20818, doi:10.1029/2005GL024164.

Lathière, J., D. A. Hauglustaine, A. D. Friend, N. De Noblet-Ducoudre, N. Viovy, and G. A. Folberth (2006), Impact of climate variability and land use changes on global biogenic volatile organic compound emissions, *Atmos. Chem. Phys.*, *6*, 2129–2146.

Lawrence, P. J., and T. N. Chase (2007), Representing a new MODIS consistent land surface in the Community Land Model (CLM 3.0), *J. Geophys. Res.*, *112*, G01023, doi:10.1029/2006JG000168.

Lee, A., A. H. Goldstein, M. D. Keywood, S. Gao, V. Varutbangkul, R. Bahreini, N. L. Ng, R. C. Flagan, and J. H. Seinfeld (2006a), Gas-phase products and secondary aerosol yields from the ozonolysis of ten different terpenes, *J. Geophys. Res.*, *111*, D07302, doi:10.1029/2005JD006437.

Lee, A., A. H. Goldstein, J. H. Kroll, N. L. Ng, V. Varutbangkul, R. C. Flagan, and J. H. Seinfeld (2006b), Gas-phase products and secondary aerosol yields from the photooxidation of 16 different terpenes, *J. Geophys. Res.*, *111*, D17305, doi:10.1029/2006JD007050.

Levis, S., C. Wiedinmyer, G. B. Bonan, and A. Guenther (2003), Simulating biogenic volatile organic compound emissions in the Community Climate System Model, *J. Geophys. Res.*, *108*(D21), 4659, doi:10.1029/2002JD003203.

Liao, H., W.-T. Chen, and J. H. Seinfeld (2006), Role of climate change in global predictions of future tropospheric ozone and aerosols, *J. Geophys. Res.*, *111*, D12304, doi:10.1029/2005JD006852.

Liggio, J., S.-M. Li, and R. McLaren (2005), Reactive uptake of glyoxal by particulate matter, *J. Geophys. Res.*, *110*, D10304, doi:10.1029/2004JD005113.

Lim, H. J., A. G. Carlton, and B. J. Turpin (2005), Isoprene forms secondary organic aerosol through cloud processing: Model simulations, *Environ. Sci. Technol.*, *39*(12), 4441–4446.

Loreto, F., P. Pinelli, F. Manes, and H. Kollist (2004), Impact of ozone on monoterpene emissions and evidence for an isoprene-like antioxidant action of monoterpenes emitted by Quercus ilex leaves, *Tree Physiol.*, *24*(4), 361–367.

Martin-Reviejo, M., and K. Wirtz (2005), Is benzene a precursor for secondary organic aerosol?, *Environ. Sci. Technol.*, *39*(4), 1045–1054.

Meehl, G. A., et al. (2006), Climate change projections for the twenty-first century and climate change commitment in the CCSM3, *J. Clim.*, *19*(11), 2597–2616.

Muller, J. F. (1992), Geographical distribution and seasonal variation of surface emissions and deposition velocities of atmospheric trace gases, *J. Geophys. Res.*, *97*(D4), 3787–3804.

Murazaki, K., and P. Hess (2006), How does climate change contribute to surface ozone change over the United States?, *J. Geophys. Res.*, *111*, D05301, doi:10.1029/2005JD005873.

Naik, V., C. Delire, and D. J. Wuebbles (2004), Sensitivity of global biogenic isoprenoid emissions to climate variability and atmospheric CO_2, *J. Geophys. Res.*, *109*, D06301, doi:10.1029/2003JD004236.

Nakicenov, N., et al. (2000), *Emissions Scenarios: A Special Report of Working Group III of the Intergovernmental Panel on Climate Change*, 599 pp, Cambridge Univ. Press, Cambridge, U. K.

Ng, N. L., J. H. Kroll, A. W. H. Chan, P. S. Chhabra, R. C. Flagan, and J. H. Seinfeld (2007a), Secondary organic aerosol formation from m-xylene, toluene and benzene, *Atmos. Chem. Phys.*, *7*, 3909–3922.

Ng, N. L., et al. (2007b), Effect of NOx level on secondary organic aerosol (SOA) formation from the photooxidation of terpenes, *Atmos. Chem. Phys.*, *7*, 5159–5179.

Odum, J. R., T. P. W. Jungkamp, R. J. Griffin, H. J. L. Forstner, R. C. Flagan, and J. H. Seinfeld (1997), Aromatics, reformulated gasoline, and atmospheric organic aerosol formation, *Environ. Sci. Technol.*, *31*(7), 1890–1897.

Offenberg, J. H., T. E. Kleindienst, M. Jaoui, M. Lewandowski, and E. O. Edney (2006), Thermal properties of secondary organic aerosols, *Geophys. Res. Lett.*, *33*, L03816, doi:10.1029/2005GL024623.

Olivier, J. G. J., et al. (1996), Description of EDGAR version 2.0: A set of global emission inventories of greenhouse gases and ozone-depleting substances for all anthropogenic and most natural sources on a per country basis and on a 1×1 degree grid, Natl. Inst. of Public Health and Environ., Bilthoven, Netherlands.

Pankow, J. F. (1994), An absorption model of the gas aerosol partitioning involved in the formation of secondary organic aerosol, *Atmos. Environ.*, *28*(2), 189–193.

Possell, M., C. N. Hewitt, and D. J. Beerling (2005), The effects of glacial atmospheric CO_2 concentrations and climate on isoprene emissions by vascular plants, *Global Change Biol.*, *11*(1), 60–69.

Presto, A. A., K. E. H. Hartz, and N. M. Donahue (2005), Secondary organic aerosol production from terpene ozonolysis. 2. Effect of NOx concentration, *Environ. Sci. Technol.*, *39*(18), 7046–7054.

Pun, B. K., and C. Seigneur (2007), Investigative modeling of new pathways for secondary organic aerosol formation, *Atmos. Chem. Phys.*, *7*(9), 2199–2216.

Purves, D. W., J. P. Caspersen, P. R. Moorcroft, G. C. Hurtt, and S. W. Pacala (2004), Human-induced changes in US biogenic volatile organic compound emissions: Evidence from long-term forest inventory data, *Global Change Biol.*, *10*(10), 1737–1755.

Rasch, P. J., N. M. Mahowald, and B. E. Eaton (1997), Representations of transport, convection, and the hydrologic cycle in chemical transport models: Implications for the modeling of short-lived and soluble species, *J. Geophys. Res.*, *102*(D23), 28,127–28,138.

Sanderson, M. G., C. D. Jones, W. J. Collins, C. E. Johnson, and R. G. Derwent (2003), Effect of Climate Change on Isoprene Emissions and Surface Ozone Levels, *Geophys. Res. Lett.*, *30*(18), 1936, doi:10.1029/2003GL017642.

Schultz, M. G., A. Heil, J. Hoelzemann, A. Spessa, K. Thonicke, J. Goldammer, A. Held, J. M. Pereira, and M. van het Bolscher (2008), Global wildland fire emissions from 1960 to 2000, *Global Biogeochem. Cycles*, doi:10.1029/2007GB003031, in press.

Shim, C., Y. Wang, Y. Choi, P. I. Palmer, D. S. Abbot, and K. Chance (2005), Constraining global isoprene emissions with Global Ozone Monitoring Experiment (GOME) formaldehyde column measurements, *J. Geophys. Res.*, *110*, D24301, doi:10.1029/2004JD005629.

Song, C., K. S. Na, and D. R. Cocker (2005), Impact of the hydrocarbon to NOx ratio on secondary organic aerosol formation, *Environ. Sci. Technol.*, *39*(9), 3143–3149.

Stevenson, D. S., C. E. Johnson, W. J. Collins, R. G. Derwent, and J. M. Edwards (2000), Future estimates of tropospheric ozone radiative forcing and methane turnover: The impact of climate change, *Geophys. Res. Lett.*, *27*(14), 2073–2076.

Sullivan, A. P., R. E. Peltier, C. A. Brock, J. A. de Gouw, J. S. Holloway, C. Warneke, A. G. Wollny, and R. J. Weber (2006), Airborne measurements of carbonaceous aerosol soluble in water over northeastern United States: Method development and an investigation into water-soluble organic carbon sources, *J. Geophys. Res.*, *111*, D23S46, doi:10.1029/2006JD007072.

Takekawa, H., H. Minoura, and S. Yamazaki (2003), Temperature dependence of secondary organic aerosol formation by photo-oxidation of hydrocarbons, *Atmos. Environ.*, *37*(24), 3413–3424.

Takemura, T., H. Okamoto, Y. Maruyama, A. Numaguti, A. Higurashi, and T. Nakajima (2000), Global three-dimensional simulation of aerosol optical thickness distribution of various origins, *J. Geophys. Res.*, *105*(D14), 17,853–17,873.

Tao, Z., and A. K. Jain (2005), Modeling of global biogenic emissions for key indirect greenhouse gases and their response to atmospheric CO_2 increases and changes in land cover and climate, *J. Geophys. Res.*, *110*, D21309, doi:10.1029/2005JD005874.

Tie, X., G. Brasseur, L. Emmons, L. Horowitz, and D. Kinnison (2001), Effects of aerosols on tropospheric oxidants: A global model study, *J. Geophys. Res.*, *106*(D19), 22,931–22,964.

Tie, X., S. Madronich, S. Walters, D. P. Edwards, P. Ginoux, N. Mahowald, R. Zhang, C. Lou, and G. Brasseur (2005), Assessment of the global impact of aerosols on tropospheric oxidants, *J. Geophys. Res.*, *110*, D03204, doi:10.1029/2004JD005359.

Tsigaridis, K., and M. Kanakidou (2003), Global modelling of secondary organic aerosol in the troposphere: a sensitivity analysis, *Atmos. Chem. Phys.*, *3*, 1849–1869.

Tsigaridis, K., and M. Kanakidou (2007), Secondary organic aerosol importance in the future atmosphere, *Atmos. Environ.*, *41*, 4682–4692.

Tsigaridis, K., et al. (2006), Change in global aerosol composition since preindustrial times, *Atmos. Chem. Phys.*, *6*, 5143–5162.

Turpin, B. J., and H. J. Lim (2001), Species contributions to PM2.5 mass concentrations: Revisiting common assumptions for estimating organic mass, *Aerosol Sci. Technol.*, *35*(1), 602–610.

van het Bolscher, M., et al. (2007), Reanalysis of the tropospheric chemical composition over the past 40 years. A long-term global modeling study of tropospheric chemistry funded under the 5th EU framework programme, *EU-Contract EVK2-CT-2002-00170*, Eur. Union, Brussels. (Available at http://retro.enes.org/reports/D1-6_final.pdf)

Velikova, V., P. Pinelli, S. Pasqualini, L. Reale, F. Ferranti, and F. Loreto (2005), Isoprene decreases the concentration of nitric oxide in leaves exposed to elevated ozone, *New Phytol.*, *166*(2), 419–426.

Volkamer, R., J. L. Jimenez, F. San Martini, K. Dzepina, Q. Zhang, D. Salcedo, L. T. Molina, D. R. Worsnop, and M. J. Molina (2006), Secondary organic aerosol formation from anthropogenic air pollution: Rapid and higher than expected, *Geophys. Res. Lett.*, *33*, L17811, doi:10.1029/2006GL026899.

Wesely, M. L. (1989), Parameterization of surface resistances to gaseous dry deposition in regional scale numerical models, *Atmos. Environ.*, *23*(6), 1293–1304.

Zeng, G., and J. A. Pyle (2003), Changes in tropospheric ozone between 2000 and 2100 modeled in a chemistry-climate model, *Geophys. Res. Lett.*, *30*(7), 1392, doi:10.1029/2002GL016708.

J. Feddema, Department of Geography, University of Kansas, Lawrence, KS 66045, USA.

I. Fung and A. H. Goldstein, Department of Environmental Science, Policy and Management, University of California, Berkeley, CA 94720, USA.

A. Guenther, P. G. Hess, J.-F. Lamarque, and F. Vitt, National Center for Atmospheric Research, Boulder, CO 80307, USA.

C. L. Heald, Department of Atmospheric Science, Colorado State University, Fort Collins, CO 80524, USA. (heald@atmos.colostate.edu)

D. K. Henze and J. H. Seinfeld, Department of Chemical Engineering, California Institute of Technology, Pasadena, CA 91125, USA.

L. W. Horowitz, Geophysical Fluid Dynamics Laboratory, NOAA, Princeton, NJ 80540, USA.